

DOI: [10.29026/oea.2024.230171](https://doi.org/10.29026/oea.2024.230171)

Miniature tunable Airy beam optical meta-device

Jing Cheng Zhang^{1†}, Mu Ku Chen^{1,2,3†}, Yubin Fan^{1†}, Qinmiao Chen^{4†},
Shufan Chen¹, Jin Yao¹, Xiaoyuan Liu¹, Shumin Xiao^{4*} and
Din Ping Tsai^{1,2,3*}

¹Department of Electrical Engineering, City University of Hong Kong, Kowloon, Hong Kong SAR 999077, China; ²State Key Laboratory of Terahertz and Millimeter Waves, City University of Hong Kong, Kowloon, Hong Kong SAR 999077, China; ³Centre for Biosystems, Neuroscience, and Nanotechnology, City University of Hong Kong, Kowloon, Hong Kong SAR 999077, China; ⁴Ministry of Industry and Information Technology Key Lab of Micro-Nano Optoelectronic Information System, Guangdong Provincial Key Laboratory of Semiconductor Optoelectronic Materials and Intelligent Photonic Systems, Harbin Institute of Technology, Shenzhen 518055, China.

[†]These authors contributed equally to this work.

*Correspondence: SM Xiao, E-mail: shumin.xiao@hit.edu.cn; DP Tsai, E-mail: dptsai@cityu.edu.hk

This file includes:

[Section 1: Simulation setup for the nanoantenna design.](#)

[Section 2: The phase combinations of the two metasurfaces.](#)

[Section 3: Nanofabrication processes of metasurfaces](#)

[Section 4: Experimental setup for characterization of the dynamic Airy beam meta-device.](#)

[Section 5: Applying the meta-device in practice.](#)

Supplementary information for this paper is available at <https://doi.org/10.29026/oea.2024.230171>



Open Access This article is licensed under a Creative Commons Attribution 4.0 International License.

To view a copy of this license, visit <http://creativecommons.org/licenses/by/4.0/>.

© The Author(s) 2024. Published by Institute of Optics and Electronics, Chinese Academy of Sciences.

Section 1: Simulation setup for the nanoantenna design

To conduct simulations for the nanoantenna design, we utilize the COMSOL Multiphysics® commercial simulation software to execute comprehensive analyses. The procedure involves nanopillar structures with varying radii ranging from 50 to 113 nm. The nanoantennas possess a fixed height of 800 nm. The simulation setup includes periodic boundary conditions along the x - and y -axes, while the z -direction incorporates a perfect matching layer (PML) boundary. A uniform mesh with a size of 30 nm is employed in all three directions (x , y , and z) within a single unit cell.

Section 2: The phase combinations of the two metasurfaces

When light passes through two metasurfaces, it will be tailored by these two metasurfaces. As we rotate the metasurfaces, the direction of the Airy beam's sidelobes shifts due to the rotation of the cubic phase profile. The off-axis Fresnel lens phase profiles on the two metasurfaces combine to generate gradient phases of various directions and magnitudes. This further allows for the manipulation of the transmission trajectory of the Airy beam.

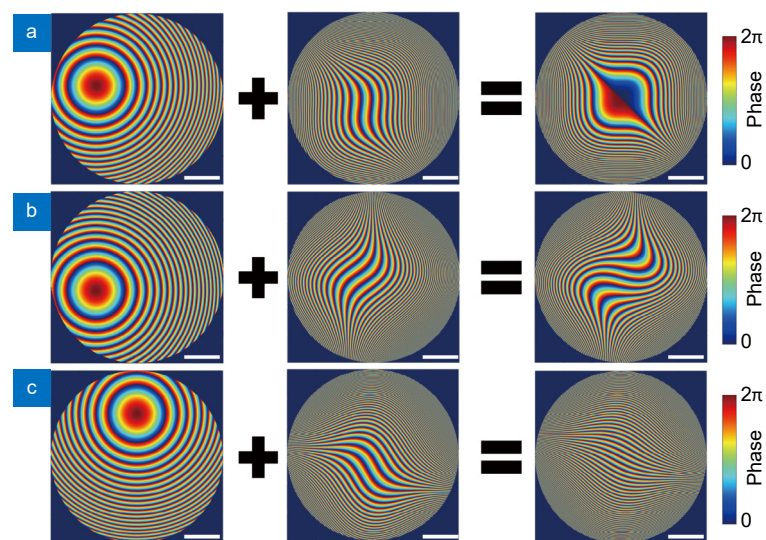


Fig. S1 | Illustration of how phase profiles merge within a single metasurface for advanced functions. The phase combinations of the first metasurface (the left column) and the second metasurface (the middle column) determine the phase (the right column) manipulating the incident light.

Section 3: Nanofabrication processes of metasurfaces

The sample was fabricated on 800 nm thick titanium dioxide (TiO_2) film with a quartz substrate. The Zep 520A photoresist layer is a spin coating on TiO_2 film. Then, the sample is exposed to electron-beam lithography (EBL, Raith E-line Plus), and the patterns are developed in the developing solution. Next, an electron-gun evaporator (Syskey, 30 kV acceleration voltage) deposits a 23 nm thick Cr layer as a hard mask on the sample. The lift-off process is done in the PG remover solution at 80 °C. Subsequently, the patterns are transferred into TiO_2 film by reactive ion etching (RIE, Oxford RIE800 Plus). The final sample is obtained by removing the residual Cr hard mask.

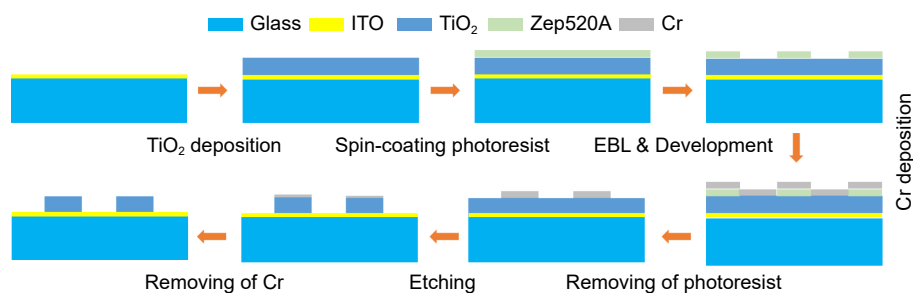


Fig. S2 | Nanofabrication processes of metasurfaces.

Section 4: Experimental setup for characterization of the dynamic Airy beam meta-device

The experimental setup is shown in Fig. S3. The 532 nm light source is generated by MGL-III-532-50mW from Hon Kok Technology Co. The lenses L1 and L2 are used for light expansion. An Objective lens (0.14 NA, 5x) and a camera on the motorized stage are used to capture the Airy beam light field.

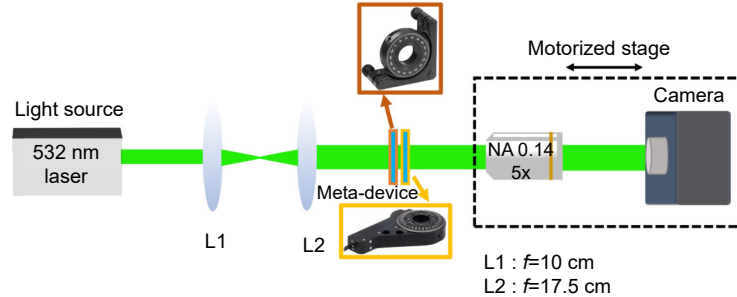


Fig. S3 | Experimental setup for characterization of the dynamic Airy beam meta-device. Inserts show the holders of the two metasurfaces to control their rotations. The left is a Kinematic Rotation Mount (KS1RS, Thorlabs Inc.), and the other is a Motorized Precision Rotation Stage (PRM1Z8, Thorlabs Inc.).

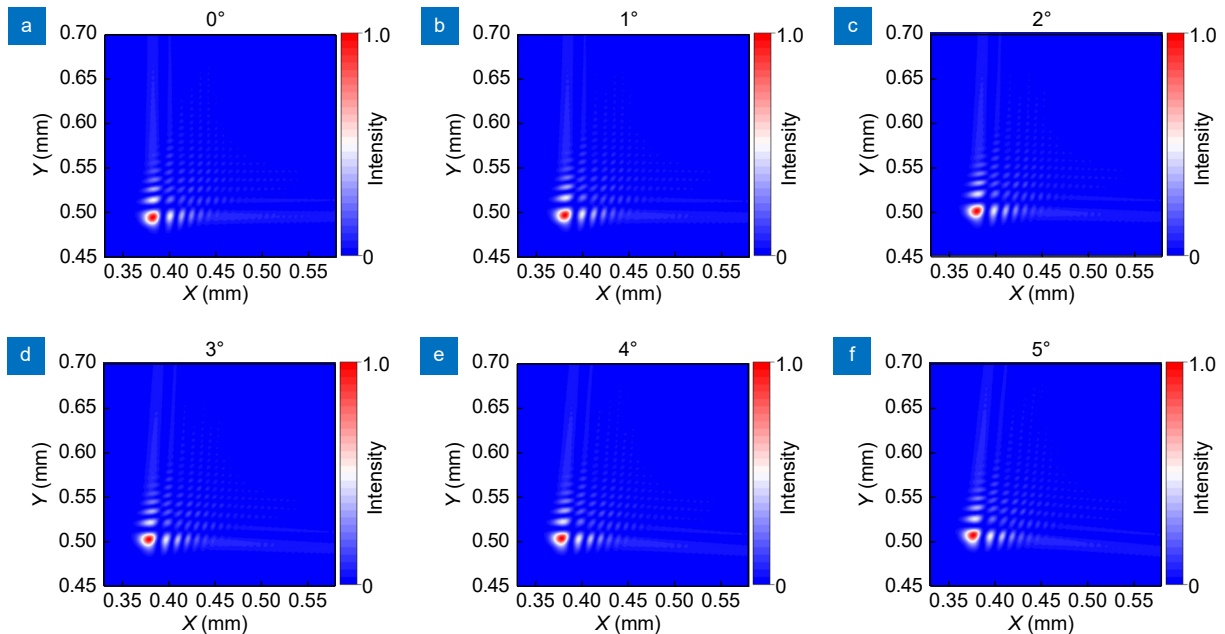


Fig. S4 | Analysis of the robustness of bilayer metasurface to the rotation angle. (a-f) The intensity distribution of the focal plane distributions as the first metasurface rotates more angles ranging from 0 to 5 degrees and other configurations is the same as shown in Fig. 3(a). As the rotation of the first metasurface will influence both the gradient and the cubic phase, thus it is more sensitive to the rotation angle. The results indicate the position of the focal spot with little change under a slight rotation shift.

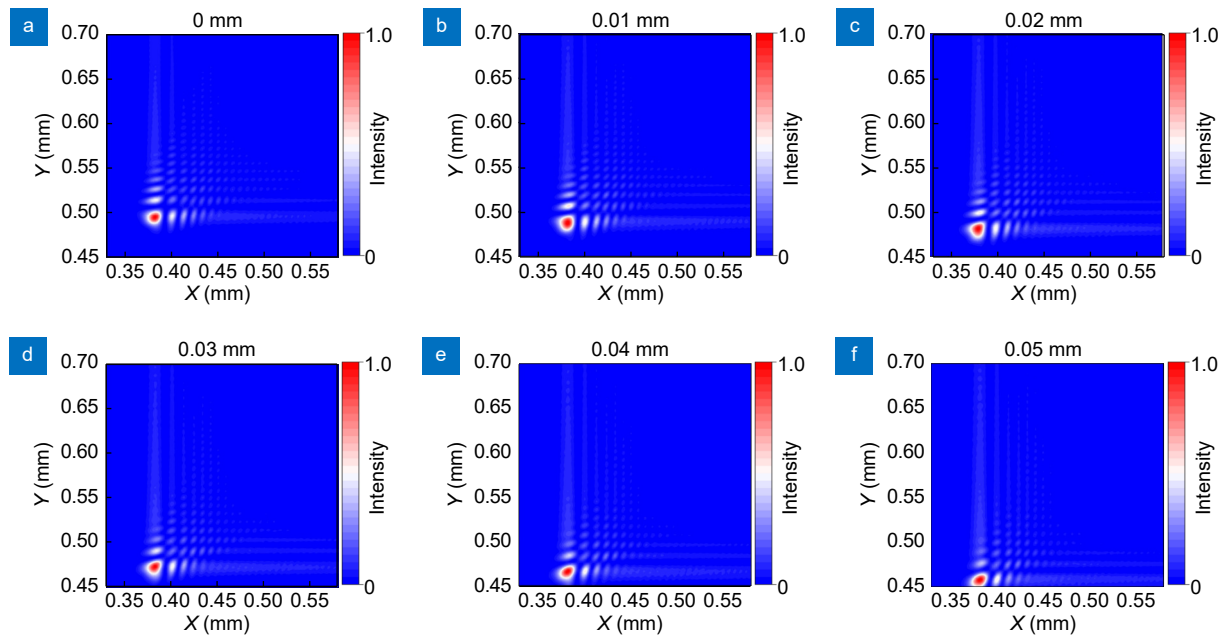


Fig. S5 | Analysis of the robustness of bilayer metasurface to the transverse shift. (a–f) The intensity distribution of the focal plane distributions as the transverse shift of the metasurfaces ranging from 0 to 0.05 mm and other configurations is the same, as shown in Fig. 3(a). The results indicate the position of the focal spot with little change under a slight shift.

Section 5: Applying the meta-device in practice

To ensure the device's performance stability, we can initially input the measured values of the relationship between the metasurfaces' rotation angles and the positions of the Airy beam's focal spots (Table S1) into the computer. Subsequently, a piezoelectric control apparatus can be employed to manipulate the rotation of the two cascading metasurfaces. This approach enables us to achieve controlled, precise, and real-time dynamic manipulation of the Airy beam.

Table S1 | Handbook for Airy beam manipulation.

$\theta_1(^{\circ})$	$\theta_2(^{\circ})$	x(mm)	y(mm)	$\theta_1(^{\circ})$	$\theta_2(^{\circ})$	x(mm)	y(mm)	$\theta_1(^{\circ})$	$\theta_2(^{\circ})$	x(mm)	y(mm)	$\theta_1(^{\circ})$	$\theta_2(^{\circ})$	x(mm)	y(mm)
0	0	-0.06	-0.03	0	90	0.15	-0.08	0	180	0.18	0.08	0	270	-0.01	0.13
60	0	-0.08	-0.08	60	90	0.13	-0.14	60	180	0.16	0.04	60	270	-0.03	0.08
120	0	-0.13	-0.09	120	90	0.08	-0.13	120	180	0.1	0.03	120	270	-0.09	0.07
180	0	-0.17	-0.05	180	90	0.04	-0.08	180	180	0.07	0.07	180	270	-0.12	0.11
240	0	-0.15	0.03	240	90	0.07	-0.04	240	180	0.1	0.12	240	270	-0.1	0.17
300	0	-0.09	0.02	300	90	0.12	-0.06	300	180	0.15	0.13	300	270	-0.05	0.18
0	22.5	-0.03	-0.08	0	112.5	0.18	-0.05	0	202.5	0.14	0.13	0	292.5	-0.05	0.09
60	22.5	-0.05	-0.13	60	112.5	0.16	-0.1	60	202.5	0.12	0.08	60	292.5	-0.07	0.04
120	22.5	-0.11	-0.14	120	112.5	0.11	-0.11	120	202.5	0.06	0.07	120	292.5	-0.13	0.04
180	22.5	-0.14	-0.1	180	112.5	0.07	-0.07	180	202.5	0.03	0.11	180	292.5	-0.16	0.08
240	22.5	-0.12	-0.05	240	112.5	0.09	-0.02	240	202.5	0.05	0.16	240	292.5	-0.14	0.12
300	22.5	-0.06	-0.04	300	112.5	0.15	-0.01	300	202.5	0.11	0.17	300	292.5	-0.09	0.13
0	45	0.01	-0.11	0	135	0.19	0	0	225	0.09	0.15	0	315	-0.06	0.05
60	45	0	-0.16	60	135	0.17	-0.05	60	225	0.06	0.1	60	315	-0.08	0
120	45	-0.06	-0.17	120	135	0.12	-0.06	120	225	0.01	0.09	120	315	-0.14	0
180	45	-0.1	-0.12	180	135	0.08	-0.01	180	225	-0.02	0.14	180	315	-0.17	0.04
240	45	-0.07	-0.07	240	135	0.1	0.03	240	225	0	0.19	240	315	-0.15	0.08
300	45	-0.02	-0.06	300	135	0.16	0.04	300	225	0.06	0.2	300	315	-0.1	0.09
0	67.5	0.08	-0.11	0	157.5	0.16	0.04	0	247.5	0.03	0.15	0	337.5	-0.07	0
60	67.5	0.06	-0.16	60	157.5	0.17	-0.01	60	247.5	0.01	0.1	60	337.5	-0.09	-0.04
120	67.5	0.01	-0.17	120	157.5	0.12	-0.12	120	247.5	-0.04	0.09	120	337.5	-0.14	-0.05
180	67.5	-0.01	-0.13	180	157.5	0.09	0.02	180	247.5	-0.07	0.14	180	337.5	-0.18	-0.01
240	67.5	0	-0.07	240	157.5	0.1	0.07	240	247.5	-0.06	0.19	240	337.5	-0.16	0.03
300	67.5	0.06	-0.06	300	157.5	0.16	0.08	300	247.5	0	0.19	300	337.5	-0.1	0.05